

A Method for Determining the Length of FBG Sensors Accurately

Aydin Rajabzadeh^{ID}, Richard Heusdens^{ID}, Richard C. Hendriks^{ID}, and Roger M. Groves^{ID}

Abstract—In this letter, we propose a method for estimating the length of single-mode fiber Bragg grating type sensors with high accuracy. Our method is based on calculating the maximum oscillation frequency of the side-lobes of the FBG reflection spectrum. We show that this frequency is independent of the stress field to which the sensor is subjected, and is dependent on the length of the sensor. This method can be used to characterize the gauge length of already installed FBG sensors so that they can provide useful data for engineering models of structural integrity. All the analyses are based on the approximated transfer matrix model, which is a newly developed numerical method for the analysis of the FBG reflection spectrum under various stress fields.

Index Terms—Fiber Bragg grating, FBG, length determination, reflection spectrum, structural integrity.

I. INTRODUCTION

FIBER Bragg grating (FBG) sensors are produced by creating a predetermined modulation in the refractive index of the optical fiber's core, for lengths typically between a few millimeters to a few centimeters. This length of refractive index modulation (grating) is the active length of the FBG sensor, which partially reflects certain wavelengths of the input light in the optical fiber. The main application of FBG sensors is in point strain or temperature sensing, and in vibration and pressure sensing [1]. Since FBG sensors are generally only locally sensitive, it is crucial to know the active length of the sensors. Due to the small diameter of the optical fiber (usually in the order of 125 μm or less), it is not possible to inspect the position of the sensor and its length without special equipment. Usually, the approximate position of the sensor is marked on the optical fiber by the producing company.

Manuscript received November 27, 2018; accepted January 1, 2019. Date of publication January 4, 2019; date of current version January 16, 2019. This work was supported by the TKI Smart Sensing for Aviation Project through the Dutch Ministry of Economic Affairs. (*Corresponding author: Aydin Rajabzadeh.*)

A. Rajabzadeh is with the Circuits and Systems Group, Electrical Engineering Faculty, Delft University of Technology, 2628 CD Delft, The Netherlands, and also with the Structural Integrity and Composites Group, Aerospace Faculty, Delft University of Technology, 2628 CD Delft, The Netherlands (e-mail: a.rajabzadehdizaji@tudelft.nl).

R. Heusdens and R. C. Hendriks are with the Circuits and Systems Group, Electrical Engineering Faculty, Delft University of Technology, 2628 CD Delft, The Netherlands (e-mail: r.heusdens@tudelft.nl; r.c.hendriks@tudelft.nl).

R. M. Groves is with the Structural Integrity and Composites Group, Aerospace Faculty, Delft University of Technology, 2629 HS Delft, The Netherlands (e-mail: r.m.groves@tudelft.nl).

Color versions of one or more of the figures in this letter are available online at <http://ieeexplore.ieee.org>.

Digital Object Identifier 10.1109/LPT.2019.2891009

However, sometimes the information regarding the exact active gauge length of the sensor is not available, is not accurate enough, or is not reported in the datasheet of the sensor, and once the sensor is embedded in a structure, it is usually impossible to visually inspect the sensor element. In this study, we propose a method to determine the active length of the sensor accurately, and we will show that the results are not affected by subjecting the sensors to different stress fields, making the method suitable for on-site and remote length determination applications.

It has already been known from the literature that for an unstressed uniform FBG, the oscillation frequency of the side-lobes of the reflection spectrum linearly depends on the length of the FBG [2]. However, to our knowledge, there have not been any studies on analyzing the sensitivity of the aforementioned oscillation frequency to parameters other than the FBG length, and also retrieving the length of non-uniformly grating or partially apodized FBG sensors under stress (uniform or non-uniform). Our method is based on the approximated transfer matrix model [3], which is a model for the analysis of FBG reflection spectra under non-uniform (and uniform) stress fields. A direct result of this model was to show that it is possible to approximate the side-lobes of the FBG reflection spectra with a closed-form representation. From this closed-form expression, it can be seen that the highest oscillation frequency of the side-lobes (which is generally the dominant frequency) linearly depends on the length of the sensor, and the effective refractive index of the fundamental core mode. In this letter, we will exploit this phenomenon to estimate the length of the sensor, and show the robustness of this approach under non-uniform and transverse stress fields.

II. CLOSED FORM APPROXIMATION OF THE SIDE-LOBES OF FBG REFLECTION SPECTRUM

A common way to analyze the FBG reflection spectrum under non-uniform stress fields is to use the transfer matrix method, where the length of the sensor is assumed to be divided to a series of piece-wise uniform segments, and then to describe the interaction of these segments using numerical methods. In 1989, Yamada and Sakuda formulated the transfer matrices, in which the interaction between the forward and backward electric waves in the core of the waveguide were described [4]. Based on the classic transfer matrix model (TMM), we proposed an approximated transfer matrix model (ATMM) [3], which offers a simpler and more compact representation of the transfer matrices in the TMM. Similar to

the TMM, for the ATMM we divide the length L of the sensor into M smaller piece-wise uniform segments of equal length of Δz , and denote the forward propagating electric wave at segment i as A_i and the backward propagating electric wave as B_i . For a small enough Δz , we showed that [3],

$$\begin{pmatrix} A_M \\ B_M \end{pmatrix} = F \begin{pmatrix} A_0 \\ B_0 \end{pmatrix}, \quad \text{in which } F = \prod_{i=1}^M F_i, \quad (1)$$

with

$$F_i = \begin{pmatrix} e^{-j(\alpha - \alpha_i)} & -j\kappa_i \Delta z \operatorname{sinc}(\alpha - \alpha_i) \\ j\kappa_i \Delta z \operatorname{sinc}(\alpha - \alpha_i) & e^{j(\alpha - \alpha_i)} \end{pmatrix}. \quad (2)$$

F_i is the approximated transfer matrix of segment i . Further, κ_i is the coupling coefficient between the forward and backward waves,

$$\alpha = \frac{2\pi n_{\text{eff}} \Delta z}{\lambda} \quad \text{and} \quad \alpha_i = \frac{2\pi n_{\text{eff}} \Delta z}{\lambda_i}. \quad (3)$$

In these relations, λ is the wavelength range under analysis, λ_i is the Bragg wavelength of the i 'th segment, and n_{eff} is the effective refractive index of the fundamental core mode. Therefore, α can be considered as a representation of the frequency under analysis, and the α_i 's as scaled local Bragg frequencies. With the assumption that there is full transmission of the incident light in the last segment and no reflection from further along the length of the sensor, i.e., $A_0 = 1$ and $B_0 = 0$, the reflection spectrum can be calculated as

$$R(\lambda) = \left| \frac{B_M}{A_M} \right|^2 = \left| \frac{F_{21}}{F_{11}} \right|^2. \quad (4)$$

where F_{11} and F_{21} are the elements of the composite matrix F given in (1). We now consider that an arbitrary axial non-uniform stress field is applied to the length of the sensor. In [3] we showed that under such conditions, for wavelengths λ that are sufficiently far away from the Bragg wavelength λ_B , the reflection spectrum can be approximated by

$$R(\lambda) \approx \left| \sum_{i=1}^{M-1} (\xi_i - \xi_{i+1}) e^{-j\left((M-2i)\alpha + \sum_{k \leq i} \alpha_k - \sum_{k > i} \alpha_k\right)} + \left(\xi_M e^{jM(\alpha - \bar{\alpha})} - \xi_1 e^{-jM(\alpha - \bar{\alpha})} \right) \right|^2, \quad (5)$$

where $\bar{\alpha} = \sum_{i=1}^M \alpha_i / M$, and $\xi_i = \frac{\kappa_i \Delta z}{2j(\alpha - \alpha_i)}$. The particular λ range in which the approximation in (5) holds, corresponds to the side-lobes of the reflection spectra.

As seen from (5), the maximum oscillation frequency of the side-lobes of the FBG reflection spectrum is $2M\alpha$, and all the other harmonics that appear in the side-lobes have lower oscillation frequencies. The $2M\alpha$ harmonic always has a fairly high amplitude, especially in wavelength regions where the $(\xi_i - \xi_{i+1})$ terms in (5) are sufficiently damped. In this region, which is associated with side-lobes with lower amplitudes, the dominant harmonic in (5) will be $2M\alpha$, and (5) can be approximated as [3]

$$R(\lambda) \approx |\xi_1|^2 + |\xi_M|^2 - 2\operatorname{Re}[\xi_1 \xi_M^*] \cos(2M(\alpha - \bar{\alpha})). \quad (6)$$

In (6) all the lower frequency harmonics that result from imperfections in the production of the sensor, and from the non-uniform stress field to which the sensor is subjected, have been neglected. As mentioned before, using (3), it can be seen from (6) that the dominant oscillating term is $\cos(2\pi 2M n_{\text{eff}} \Delta z (\frac{1}{\lambda} - \frac{1}{\lambda_B}))$. Therefore, considering the fact that $L = M \Delta z$, the maximum oscillation frequency is $f_{\text{max}} = 2 L n_{\text{eff}}$, which only depends on the length of the sensor L and the effective refractive index of the core. Our method of determining the length of FBG sensors is based on exploiting this phenomenon and retrieving the length of the sensor from this maximum oscillation frequency. However, we first need to analyze the sensitivity of " f_{max} " to the effective refractive index of the core.

III. FBG LENGTH DETERMINATION

Commercial FBG sensors are usually inscribed in single mode optical fibers, whose effective refractive index are usually in the order of $n_{\text{eff}} \approx 1.45$. In fact, the most common optical fiber for FBG inscription is the SMF28 with $n_{\text{eff}} \approx 1.447$ [5]. An example of a fiber with a higher refractive index is the PR2008 fiber with $n_{\text{eff}} \approx 1.453$ [5]. As it can be seen from these figures, the difference between the initial effective refractive index of different types of single mode optical fibers are less than 0.2%. Furthermore, during the inscription of the gratings on an optical fiber, the changes of the refractive index of the fundamental core mode is less than $\Delta n_{\text{DC}} \leq 2.5 \times 10^{-3}$, even under long exposure times and high input pulse energies [6]. This DC effective refractive index change is significantly larger for sensors that are produced by exposure to femto-second laser pulses. They are in the order of around $\Delta n_{\text{DC}} \leq 6 \times 10^{-3}$ [7]. This means that the sensitivity of the dominant oscillation frequency in (6) to the variations of the refractive index of the core is less than 1%. Therefore, without having any knowledge about the type of the optical fiber in use, the exposure time or the pulse energy of the FBG production process, or even the method of production, the maximum error in length determination that is introduced by setting a conventional fixed value for n_{eff} is at most less than 1%. This makes the method reliable for blind measurements of the length of FBG sensors, without any prior knowledge about the origin of the sensor.

Another factor that needs to be considered here is the effect of transverse loads and birefringence effects. Birefringence can be caused by external perturbations such as transverse loads or bending of the fiber. In addition, birefringence can affect the FBG sensor during production. In either scenario, the result is that the propagating light along the length of the fiber experiences different refractive indices along the slow and fast polarization axes. Under these conditions, the overall reflection spectrum of the disturbed FBG will be

$$R(\lambda) = R_x(\lambda) + R_y(\lambda), \quad (7)$$

where R_x is the reflection spectrum along the x -axis and R_y is the reflection spectrum along the y -axis. In both of these polarization axes, the maximum oscillation frequency is still equal to $2L n_{\text{eff}}$. Therefore, the maximum frequency of the side-lobes of the summation term given in (7) will also be equal to $2L n_{\text{eff}}$.

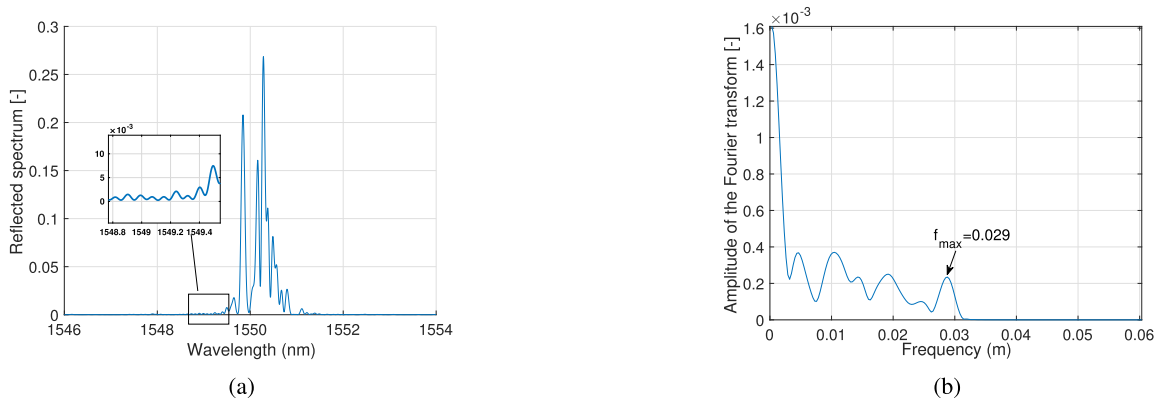


Fig. 1. (a) A simulated FBG sensor with refractive index fluctuations under an extremely non-uniform strain field, with both transverse and axial components, and (b) Fourier transform of the side-lobes given in (a).

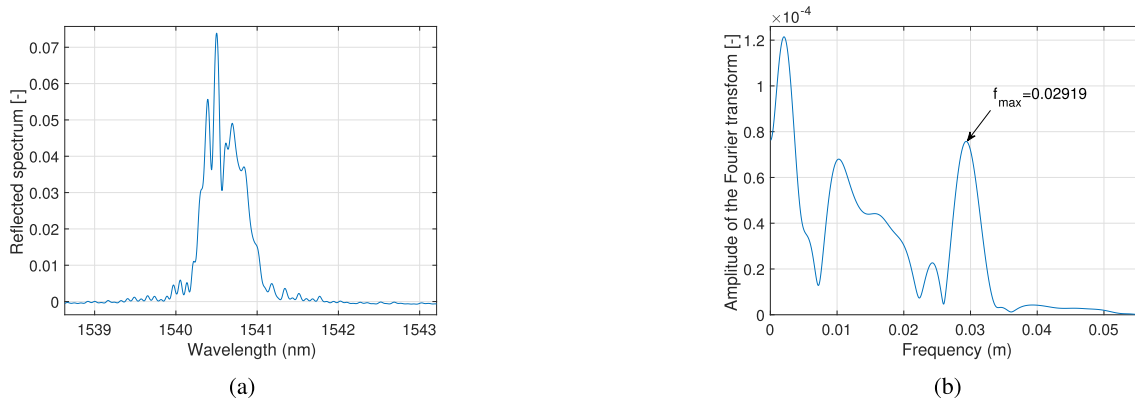


Fig. 2. (a) Reflection spectrum of an actual FBG sensor under an extremely non-uniform strain field, with both transverse and axial components, and (b) Fourier transform of the side-lobes given of the reflection spectrum.

Based on the discussions above, it can be concluded that by inspection of the maximum frequency of the side-lobes of the FBG reflection spectra, it is possible to retrieve the length of the sensor, as this frequency linearly depends on the length of the sensor. This approach is rather insensitive to the external media to which the sensor is subjected and other physical properties of the sensor. Our method of retrieving the length of the FBG is simply to take the Fourier transform of the side-lobes of the FBG reflection spectrum, and to determine the maximum frequency at which the amplitude of the Fourier transform is above the noise level. In other words, by taking the Fourier transform of (6) and the cosine term within this equation, we expect to find high amplitude harmonics at $\delta(f \pm 2Ln_{\text{eff}})$ frequencies. Note that as mentioned before, in the side-lobes, this maximum oscillation frequency is the dominant term, and its amplitude is also relatively large compared to the lower oscillation frequencies.

IV. RESULTS AND DISCUSSION

In this section we validate our method for determining the length of FBG sensors using two experiments. In the first experiment, which is a computer simulation, we designed an FBG sensor with a nominal length of 10 mm, and applied a non-uniform stress on it with both axial and transverse components. We also included imperfections to the designed sensor by adding fluctuations in the refractive index of the core. The resulting reflection spectrum is shown in Fig. 1a.

Fig. 1b shows the amplitude of the Fourier transform of the side-lobes of this sensor (denoted by the zoomed-in rectangle in Fig. 1a). Note that the oscillation terms in (6) are described in "α" or "1/λ" domain, therefore, the unit on the x-axis of its Fourier transform will be in meters. It can be seen from the figure that the maximum dominant frequency in the Fourier transform is at $f_{\text{max}} = 0.029$ m, therefore, the length calculated based on this frequency and the given effective refractive index ($n_{\text{eff}} = 1.4469$) is $\tilde{L} = f_{\text{max}}/(2n_{\text{eff}}) = 0.01002$ m or 10.02 mm. The error of calculation in this example is therefore around 0.2%.

In the second example, we tested our method on a real FBG sensor. Fig. 2a shows the reflection spectrum of a draw tower grating (DTG) sensor with a nominal length of 10 mm under an arbitrary non-uniform strain field, with components in both axial and transverse directions. The FBG sensor used in this experiment is partially apodized, with a side-lobe suppression ratio of 10 dB. The FBG sensor was interrogated with PXIe 4844 interrogator from National Instruments with spatial resolution of 4 μm and dynamic range of 40 dB. The amplitude of the Fourier transform and the maximum frequency are shown in Fig. 2b. The same sensor underwent several other load scenarios, where the sensor was subject to various arbitrary transverse and axial loads. Those results are summarized in Table I. As it is evident from this table, the location of the highest oscillating harmonic barely changes under different force loads. In these calculations, the presumed effective refractive index of the

TABLE I
FBG SENSOR UNDER DIFFERENT STRESS FIELDS, THE RESULTING
MAXIMUM OSCILLATION FREQUENCY, AND THE RESULTING
ESTIMATED SENSOR LENGTH

Stress field	Maximum oscillation frequency (m)	Estimated sensor length (mm)
Unstressed sensor	0.02922	10.0828
Load scenario #1	0.02919	10.0725
Load scenario #2	0.02925	10.0932
Load scenario #3	0.02919	10.0725
Load scenario #4	0.02916	10.0621
Load scenario #6	0.02922	10.0828

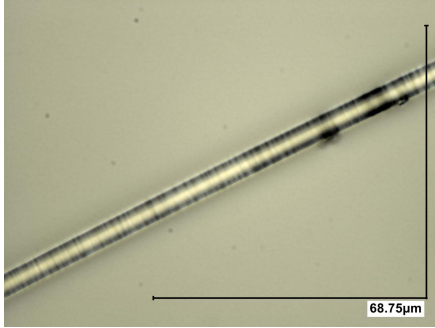


Fig. 3. A small part of the gratings structure of the optical fiber's core under an optical microscope.

core was $n_{\text{eff}} = 1.447 + 2 \times 10^{-3} = 1.449$, which was based on the assumption that the optical fiber has similar properties to the SMF28 fiber, with a DC offset of 2×10^{-3} due to being exposed to UV light.

Based on the length estimation results, the standard deviation of the estimated length is around 0.01 mm. Furthermore, since there can always be fluctuations on the specified nominal length of the sensor in the datasheet, we tried to have a more accurate reference for the validation of our method by locating the exact position of the sensor along the fiber length. The most accurate method that could offer a better accuracy than the specified nominal length was to put the optical fiber under the microscope, and to locate the gratings along the fiber length. However, due to the small refractive index modulation of the DTG sensors and the small diameter of their core, it was impossible to locate the gratings through the cladding and the coating layer. Therefore, we first mechanically removed the Ormocer coating of the fiber using a thermal stripper, and then chemically etched the fiber off its cladding layer in order to be left with only the core of the fiber. For the etching process, we used a solution of 15 wt% of NH_4F and 16 wt% of H_2SO_4 [8], and we submerged the sensor containing part of the optical fiber with an original diameter of $125 \mu\text{m}$ in the solution for a period of around 5 hours, during which time the diameter was reduced to around $10 \mu\text{m}$. Afterwards, we put the etched fiber under an optical microscope with magnification of around 2500 in order to locate the FBG length. Fig. 3 shows a small part of the grating under the microscope. Based on the microscopy results, the overall length of the sensor with significant variations in its refractive index was determined as 10.093 mm. Based on the reference values for the FBG length, in this particular example, our method offers a better accuracy for the FBG length, even

compared to the datasheet of the sensor, with a maximum error of around 0.3%.

It is noteworthy that our method could potentially perform well for other types of short Bragg grating sensors too, as long as a high dynamic range interrogator is being used and the side-lobes have not been deliberately fully suppressed (such as Gaussian apodized sensors [1]). Nevertheless, our method works perfectly well for partially apodized FBG sensors, as well as non-apodized FBG sensors. Furthermore, it can be employed for length determination of chirped FBG sensors [1], phase shifted FBG structures, and for other types of aperiodic grating structures as well.

V. CONCLUSIONS

In this letter, we showed that the length of conventional FBG sensors can be estimated based on calculating the maximum oscillation frequency of the side-lobes of the FBG reflection spectrum. We showed that this oscillation frequency is independent of the stress (or temperature) field to which the sensor is subjected, and that its sensitivity to the variations of the effective refractive index of the core is negligible, making the method reliable for FBG length determination without having a prior knowledge about the production method, optical fibers in use and etc. Furthermore, the results of our method can be extended to other types of non-uniformly grating and partially apodized FBG sensors. We used computer simulations and experimental measurements to validate our method, and the results were in line with our expectations on the presented model.

ACKNOWLEDGEMENT

This research is part of the TKI Smart Sensing for Aviation Project, sponsored by the Dutch Ministry of Economic Affairs under the Topsectoren policy for High Tech Systems and Materials, and industry partners Airbus Defence and Space, Fokker Technologies GKN Aerospace and Royal Schiphol Group.

REFERENCES

- [1] A. D. Kersey *et al.*, "Fiber grating sensors," *J. Lightw. Technol.*, vol. 15, no. 8, pp. 1442–1463, Aug. 1997.
- [2] T. Erdogan, "Fiber grating spectra," *J. Lightw. Technol.*, vol. 15, no. 8, pp. 1277–1294, Aug. 1997.
- [3] A. Rajabzadeh, R. Heusdens, R. C. Hendriks, and R. M. Groves, "Calculation of the mean strain of smooth non-uniform strain fields using conventional FBG sensors," *J. Lightw. Technol.*, vol. 36, no. 17, pp. 3716–3725, Sep. 1, 2018.
- [4] M. Yamada and K. Sakuda, "Analysis of almost-periodic distributed feedback slab waveguides via a fundamental matrix approach," *Appl. Opt.*, vol. 26, no. 16, pp. 3474–3478, 1987.
- [5] F. Juelich and J. Roths, "OP2-determination of the effective refractive index of various single mode fibres for fibre Bragg grating sensor applications," in *Proc. OPTO IRS*, 2009, pp. 119–124.
- [6] M. Bernier, S. Gagnon, and R. Vallée, "Role of the 1D optical filamentation process in the writing of first order fiber Bragg gratings with femtosecond pulses at 800 nm," *Opt. Mater. Express*, vol. 1, no. 5, pp. 832–844, 2011.
- [7] E. Fertein, C. Przygodzki, H. Delbarre, A. Hidayat, M. Douay, and P. Niay, "Refractive-index changes of standard telecommunication fiber through exposure to femtosecond laser pulses at 810 nm," *Appl. Opt.*, vol. 40, no. 21, pp. 3506–3508, 2001.
- [8] S. Ko, J. Lee, J. Koo, B. S. Joo, M. Gu, and J. H. Lee, "Chemical wet etching of an optical fiber using a hydrogen fluoride-free solution for a saturable absorber based on the evanescent field interaction," *J. Lightw. Technol.*, vol. 34, no. 16, pp. 3776–3784, Aug. 15, 2016.